THE AGES OF DISTURBED FIELD ELLIPTICAL GALAXIES. II. CENTRAL PROPERTIES

David R. Silva[1]

European Southern Observatory, Karl-Schwarzschild-Strasse 2, D-85748 Garching, Germany; dsilva@eso.org

AND

Gregory D. Bothun[1]

Department of Physics, University of Oregon, 120 Willamette Hall, Eugene, OR 97403; nuts@moo.uoregon.edu

ABSTRACT

The formation of elliptical galaxies via the merger of gas-rich disks has received considerable attention in recent years, with many studies strongly supporting the merger hypothesis. When investigated in detail, the dynamics of a major merger that produces a high phase-space density of material (e.g., the center of an elliptical galaxy) invariably produces the ubiquitous signature of a centrally concentrated burst of star formation. We have searched for this central burst of star formation in a sample of field elliptical galaxies that exhibit morphological fine structure thought to be indicative of merging. Out of this sample of 32 galaxies, we find only two galaxies, NGC 3610 and NGC 5322, with sufficiently red central near-IR colors to be consistent with the asymptotic giant branch light reflective of the central burst of star formation a few gigayears ago. Using NGC 3610 and 5322 as case studies, we discuss possible astrophysical links between global and central properties and their implied constraints on elliptical galaxy formation and evolution. In particular, we conclude that the available evidence argues against mergers of disk galaxies within the last 3–4 Gyr as being the primary formation mechanism for morphologically disturbed field elliptical galaxies.

Key words: galaxies: elliptical and lenticular, cD — galaxies: evolution — galaxies: formation — galaxies: stellar content — galaxies: structure

1. INTRODUCTION

Many current-epoch elliptical galaxies in low-density environments (so-called field ellipticals) exhibit morphological fine structure and/or the presence of kinematically unsettled features (e.g., counterrotating cores and central dust lanes). As such features can only persist for 1–3 Gyr before being destroyed via phase mixing, it has been widely suggested that they were produced by a recent merger event (see Bender et al. 1989; Schweizer & Seitzer 1992; Illingworth & Franx 1989; van Dokkum & Franx 1995; Quinn 1984; Hernquist & Quinn 1988, 1989; Barnes 1992). But is such kinematic/dynamical evidence alone sufficient to establish that most field ellipticals were indeed formed through mergers? As it would seem unlikely that dynamical features could be produced without some kind of augmentation of the stellar population, there should be an additional signature of the merger event contained in the integrated light of these galaxies.

Two possible stellar population signatures have been noted by Schweizer et al. (1990) and Schweizer & Seitzer (1992, hereafter SS92). They found that elliptical galaxies with morphological fine structure tend to have stronger central Hβ absorption and bluer integrated *UBV* colors within their effective radii than elliptical galaxies with little or no morphological fine structure. SS92 argued that both observations could be explained if these elliptical galaxies had been formed by disk-disk mergers roughly 3–5 Gyr ago, which resulted in a distributed burst of star formation.

In this scenario, the strong Hβ and blue *UBV* colors are produced by the stellar population created in this merger-driven star formation event.

However, the near-IR colors of these same galaxies present a different picture. As discussed in Silva & Bothun (1998, hereafter Paper I), their global near-IR colors place the SS92 galaxies in the same locus of points in the $J-H$ versus $H-K$ plane as elliptical galaxies with no signs of recent merger activity. This strongly constrains the global fractional amount of intermediate-age (1–3 Gyr) stellar mass to be no more than 10%–15%, and in most cases, the data are consistent with all the stellar mass being old ($T > 10$ Gyr) and metal-rich ([Fe/H] ≥ -0.3). We argued in Paper I that any recent merger activity was therefore not accompanied by a significant episode of distributed star formation within the region defined by $R < 1.5R_e$ and that the bluer *UBV* colors observed in this region for some of these galaxies are due to metallicity effects driven by the accretion of lower metallicity stars or by relative abundance differences.

The Paper I result, however, does not rule out a centrally concentrated younger stellar population. The existence of such a population in recent merger products is a ubiquitous prediction of models that include gasdynamics. In such models, the majority of the gas quickly flows to the bottom of the potential well and reaches high enough densities to trigger star formation. The preexisting stars are more uniformly distributed throughout the potential well (Negroponte & White 1983; Barnes & Hernquist 1991; Mihos, Bothun, & Richstone 1992; Mihos & Hernquist 1996; Barnes & Hernquist 1996). In the case of ultraluminous *IRAS* galaxies, large collections of central gas and associated bursts of star formation are directly observed (Mihos & Bothun 1998; Downes & Solomon 1998). We therefore would expect similar, but scaled down, levels of

---

TABLE 1
Observational Sample

NGC (1)	Σ (2)	Class (RSA) (3)	$-M_B$ (mag) (4)	A_B (mag) (5)	V_R (km s^{-1}) (6)	$\log D_N$ (7)	σ (km s^{-1}) (8)	Hot Population? (9)	Core (10)
Elliptical galaxies:									
547	...	E1	...	0.12	5524	0.59	171	...	...
596	4.60	E0	21.25	0.12	1817	0.93	151	G_T, Hβ	P
636	1.48	E1	20.76	0.10	1805	0.83	156	G_2, Hβ	...
821	...	E6	...	0.16	1716	0.86	199	...	...
1453	1.48	E2	22.26	0.24	3906	0.78	290	...	...
1700	3.70	E3	22.50	0.12	3881	0.90	233	G_2, Hβ	P
2974	0.00	E4	20.88	0.11	1924	0.95	222	...	...
3156	1.70	E5:	18.82	0.04	1296	0.68	112	G_0, Hβ	...
3193	0.00	E2	20.13	0.08	1378	0.93	205	...	...
3377	1.48	E6	19.66	0.06	689	1.06	131	G_0, Hβ	P
3379	0.00	E0	20.44	0.05	922	1.24	201	...	C
3605	2.70	E5	18.48	0.00	686	0.57	120	Hβ	P
3608	0.00	E1	19.87	0.00	1197	0.89	204	...	C
3610	7.60	E5	21.37	0.00	1765	1.02	159	G_1, Hβ	...
3640	6.85	E2	21.01	0.10	1302	1.03	176	G_T, Hβ	...
4125	6.00	E6	22.28	0.04	1340	1.11	229	G_1, Hβ	...
4168	3.00	E2	19.63	0.04	2307	0.74	182	...	C
4660	0.00	E5	19.59	0.00	1115	0.91	198	...	...
4697	0.00	E6	21.76	0.04	1210	1.22	165	G_0	P
4915	5.48	E0	21.11	0.04	3152	0.76	209	G_1, Hβ	...
5322	2.00	E4	22.14	0.00	1804	1.06	224	G_2, Hβ	...
5831	3.60	E4	20.28	0.14	1683	0.77	166	Hβ	...
S0 galaxies:									
315	...	EL	...	0.26	4956	0.82	352	...	...
584	2.78	S0$_1$(3, 5)	21.76	0.12	1875	1.06	217	Hβ	...
1023	...	SB0$_1$(5)	21.17	0.25	661	...	...	...	P
1052	1.78	E3/S0	20.89	0.06	1475	1.00	206	...	...
1172	...	S0$_1$(0, 3)	19.48	0.10	1669	0.58	121	...	P
2549	0.00	S0$_{1,2}$ (7)	19.80	0.12	1082	...	...	...	...
2685	2.48	S0$_3$(7) pec	19.55	0.15	881	...	...	...	...
2768	0.00	S0$_{1,2}$(6)	21.55	0.02	1363	1.03	198	...	...
3489	0.00	S0$_3$/Sa	19.13	0.02	659	...	...	...	...
3607	0.00	S0$_3$(3)	20.71	0.00	951	1.10	248	...	...
Ongoing merger:									
3921	8.84	Merger	...	0.00	5926	...	...	...	...

Notes.—Col. (1): NGC number. Col. (2): Morphological fine-structure parameter from SS92. Col. (3): Morphological classification from Revised Shapley-Ames Catalog (RSA; Sandage & Tammann 1981). Col. (4): Absolute B magnitude, from RSA. Col. (5): Foreground Galactic absorption from Burstein et al. 1987 or Burstein & Heiles 1984. Col. (6): Heliocentric radial velocity, from Burstein et al. 1987. Col. (7): $\log D_N$ from Burstein et al. 1987. Col. (8): Adopted central velocity dispersion, from Davies et al. 1987. Col. (9): "Hot" population indicators: Hβ = strong central Hβ absorption (Schweizer et al. 1990 or González 1993) and G = global UBV color excess indicated by SS92. Based on the discussion in SS92, galaxies are classified as follows: G_1 = possible recent (1–3 Gyr) disk-disk merger product with significant merger-driven star formation; G_2 = possible older ($\sim$5 Gyr) disk-disk merger product with significant merger-driven star formation; G_T = possible sites of recent (1–3 Gyr) star formation events induced by gas transfer only; G_0 = globally blue UBV colors but conflicting evidence about recent merger activity and/or the origin of the blue light. See SS92 for further details. Col. (10): Core morphology, as defined by Faber et al. 1997 based on *HST* observations. C = core, P = power law.

central gas collection and star formation in any elliptical galaxy that formed from a recent disk-disk merger.

Given this picture, elliptical galaxies that formed from disk-disk mergers in the last few gigayears should have central stellar populations that are younger than their outer populations. This younger population, which consists of $\sim$5% of the total remnant mass, could be quite centrally concentrated (within $r \sim 0.5$ kpc; Mihos & Hernquist 1996). This high degree of concentration makes this younger stellar population hard to detect against the background of older stars in the relatively large apertures used in Paper I. If the enhanced central Hβ lines observed by Schweizer et al. (1990) and González (1993) are caused by an intermediate-age stellar population formed 2–3 Gyr ago as suggested by SS92, then this stellar population should also include many cool asymptotic giant branch (AGB) stars above the tip of the first-ascent giant branch (FGB), as intermediate-age Magellanic Cloud clusters do (Persson

et al. 1983; Frogel, Mould, & Blanco 1990). As Persson et al. demonstrated, stellar populations that contain a significant fraction of such intermediate-age AGB stars have distinctive near-IR colors. In particular, their $H-K$ color is quite red for their $J-H$ color relative to clusters without such stars. Thus, elliptical galaxies that contain a centrally concentrated intermediate-age (1–3 Gyr) stellar population should have a significant number of bolometrically bright, cool AGB stars above the first-ascent giant branch and therefore have very red central ($r \lesssim 0.5$ kpc) integrated $H-K$ colors, relative to the colors of their outer regions, while only having slightly redder central integrated $J-H$ colors.

In this paper, a detailed study of the central near-IR colors of disturbed, current-epoch field elliptical galaxies is presented. Our sample is principally drawn from Schweizer et al. (1990), SS92, and González (1993) and concentrates on so-called field ellipticals. It includes galaxies con-

sidered to contain "young" stellar populations based on their global optical colors (SS92) and/or on central Hβ strengths (Schweizer et al. 1990; González 1993). Our goal is to determine the fraction of such galaxies that contain a centrally concentrated intermediate-age (1–3 Gyr) stellar population. Our basic methodology relies on accurate color comparisons between the central and outer regions of our sample galaxies. The *JHK* images of these galaxies discussed in Paper I provide the basis for our analysis of central colors. In broad terms, this analysis uses $J - K$ as a metallicity indicator while $H - K$, relative to $J - H$, is used to constrain the existence of cool, intermediate-age AGB stars (see also Persson et al. 1983 and Paper I). A short overview of our sample and observations is given in § 2. We explain our basic goals and methods for measuring central colors in § 3. Observational results are presented in § 4. We discuss these results and their implications for elliptical galaxy formation and evolution in § 5 and summarize our remarks in § 6.

2. OBSERVATIONS

2.1. *Galaxy Sample Characteristics*

The basic properties of our sample galaxies are presented in Table 1. Individual galaxies have been separated into elliptical ($N = 22$), S0 ($N = 10$), and merger ($N = 1$) subgroups based on their gross Revised Shapley-Ames (RSA) morphological classification (Sandage & Tammann 1981). Galaxies with the global photometric signature of a "hot" stellar component (i.e., blue *UBV* colors; SS92) are indicated by a "G" in column (9) of Table 1. These galaxies are broken down into four subgroups, based on SS92 classifications: (1) G_1 represents a possible recent (1–3 Gyr) disk-disk merger product with significant merger-driven star formation; (2) G_2 represents a possible older (~ 5 Gyr) disk-disk merger product with significant merger-driven star formation; (3) G_T represents possible sites of star formation events induced by gas transfer only; and (4) G_0 represents galaxies with globally blue colors but conflicting evidence about recent merger activity and/or the origin of the blue light. To first order, galaxies in class G_1 should have the highest probability of containing intermediate-age AGB stars. Galaxies with the central photometric signature of a "hot" stellar component (i.e., strong central Hβ absorption; Schweizer et al. 1990 or González 1993) are indicated by "Hβ" in column (9) of Table 1. Finally, the presence of a "core" or "power law" central profile as determined by *Hubble Space Telescope* (*HST*) imagery (Faber et al. 1997) is indicated in column (10).

2.2. *Data Acquisition, Reduction, and Calibration*

JHK images of the E/S0 galaxies listed in Table 1 were obtained in 1993 February with the Simultaneous Quad Infrared Imaging Device (SQIID) at the KPNO 1.3 m telescope. SQIID contained four confocal Hughes Carlsbad 256 × 256 PtSi Schottky barrier diode arrays. While these arrays had few bad pixels, low dark current, and low read noise, they also had low quantum efficiency. In principle, simultaneous acquisition of *J*-, *H*-, *K*-, and *L*-band images was possible with SQIID. In practice, only *JHK* images were acquired during this project. Each channel had a slightly different plate scale that was $\approx 1\farcs3$ pixel^{-1}, providing an almost $5\farcs5 \times 5\farcs5$ field of view. Further details about SQIID may be found in Ellis et al. (1993).

Complete details about data acquisition, reduction, and calibration may be found in Paper I. The colors reported in the current paper have been transformed to the CIT system, as defined by the Elias et al. (1982) faint standards.

3. METHODOLOGY

3.1. *Elliptical Aperture Photometry*

In Paper I, colors were measured through circular apertures. However, if morphological fine-structure results from the merger process are present in the form, for instance, of central flattened disks, then the use of elliptical apertures is more appropriate. Defining elliptical apertures requires first defining elliptical isophotes. Elliptical isophotes were fitted to each image using the algorithm described by Jedrzejewski (1987) as implemented in the STSDAS[2] ISO-PHOTE package. Implementation details are discussed in the ELLIPSE task documentation. An initial center, semimajor axis, ellipticity, and position angle were specified. Keeping only the center fixed, ellipses were then fitted to the data after rejecting the 5% brightest pixels within each ellipse sample. The median data value of each ellipse sample was computed and assigned as the isophotal value. The semimajor axis was then incremented by a factor of 1.10 (logarithmic sampling), and this process was repeated. During this process, the ellipse centers were held fixed, but their ellipticity and position angles were allowed to vary.

For each galaxy, the *JHK* images were processed separately. However, the combination of relatively short exposure times and relative *JHK* quantum efficiencies of the PtSi arrays in SQIID meant that the final *J*-band images had significantly higher signal-to-noise ratios than the final *K*-band images. Thus, we elected to define our elliptical apertures on the *J*-band images only and then apply the exact same geometric apertures to the corresponding *H* and *K* images. In this way, we were assured that we were measuring the same physical area in each photometric band.[3] The implicit assumption that the intrinsic structure of the galaxy is the same in all bands seems mostly justified. In the hypothetical case in which a recent merger has created a centrally concentrated intermediate-age stellar population whose intrinsic spatial distribution may be somewhat different than the overall ellipticity of the inner isophotes, the effect would be a slightly different isophotal structure at *K* relative to *J*. This would manifest itself as a clearly detectable color gradient in the elliptical aperture photometry.

3.2. *Simulations of Possible PSF Effects*

Since our technique rests on the reliability of color measurements made within an aperture defined by a limited number of pixels, it is important to model any possible systematic effects that could be present. Three instrumental effects could introduce systematic errors into the measurement of intragalaxy color differences: poor spatial sampling of the true point-spread function (PSF), PSF smoothing of the true central color distributions, and enhanced color dif-

---

ferences due to mismatched PSFs between the individual filter bands. Each of these effects drives the choice of the smallest reliable central aperture in a different way. Using simulated data, we have estimated the magnitude of each of these effects and what central aperture size seems prudent. The effects of PSF variations on the determination of radial color gradients measured from galaxy surface photometry have been discussed by Franx, Illingworth, & Heckman (1989) and Peletier et al. (1990).

The SQIID plate scale was roughly $1\overset{''}{.}4$ pixel^{-1}. Although the delivered image quality at the KPNO 1.3 m was never very good, it was typically under $2''$ FWHM, which SQIID did not sample very well. To study the effect of poor PSF sample, we simulated a "blue" and "red" image of a model galaxy with a known color-aperture relationship. These images were smoothed with two-dimensional circularly symmetric Gaussian functions with a range of FWHM values. The smoothed images were then sampled at two resolutions: $0\overset{''}{.}3$ pixel^{-1} and $1\overset{''}{.}4$ pixel^{-1}. Color-aperture relationships were constructed by measuring total intensity through centered circular apertures on each image and then using these intensities to calculate a color for each aperture. The results of this simulation are shown in Figure 1. As that figure shows, the effects of PSF smoothing are much larger than the effects of poor sampling on these color-aperture relationships, and both effects are negligible for apertures with $r \geq 3''$. In other words, despite the rather poor spatial sampling of SQIID, it should be possible to detect a centrally concentrated "red" stellar population as long as the actual intrinsic PSF was sufficiently small.

The magnitude of the PSF smoothing effect will vary depending the input shape of the color-aperture relation-

ship. This is illustrated in Figure 2. The top panel again illustrates the results shown in Figure 1 but for only the $1\overset{''}{.}4$ pixel^{-1} plate scale. The middle panel shows the effects of increasing PSF size on a color-aperture relationship that is more linear and less centrally concentrated than the top panel. The bottom panel shows the effects of increasing PSF size on a color-aperture relationship that is more centrally concentrated than the relationship used in the top panel. These three color-aperture relationship types effectively simulate the expected form of the color-aperture relationships of the galaxies in our sample. In each of these relationships, the effects of PSF size become negligible for apertures with $r \geq 3''$.

So far, these simulations have assumed that the "blue" and "red" images have the same PSF FWHM and that the galaxy actually has a color-aperture relationship that varies. Figure 3 illustrates what happens when these assumptions are changed. In this simulation, we have used a model galaxy with a flat color-aperture relationship. In the top panel, the effects of increasing the "red" PSF FWHM while keeping the "blue" PSF FWHM constant are shown. In the bottom panel, the effects of increasing the "blue" PSF FWHM while keeping the "red" PSF FWHM constant are shown. A PSF FWHM difference as small as 10% can create significant central-color measurement errors, and these errors become larger as PSF size differences increase. Furthermore, the radial range over which these effects are significant increases as PSF FWHM differences increase.

One can, of course, directly determine how well the individual PSF sizes match if suitable stars are within the galaxy images. Unfortunately, not all our galaxy images contain stars with high enough signal-to-noise ratios to determine accurately PSF size in all bands. For galaxies where bright-enough stars are available, the *maximum* variation seen is about 25%, which implies possible systematic color errors for $r \leq 5''$. More typically, the observed variations are at the 10% level, implying possible systematic color errors within $3''$.

In SQIID, interband PSF variations could arise from a slight interchannel nonconfocality and slight registration errors between the individual images combined to form the final image. The first variance changed in magnitude depending on focus accuracy. The only remedy was to maintain focus as accurately as possible. We assessed the magnitude of the second variance by measuring the color-aperture relationship on the individual images that were combined to form the final image and then comparing those individual measurements with the mean color-aperture relationship measured from the final image. Data sets were rejected from this study if the mean color-aperture relationship varied significantly from the individual color-aperture relationships at small radii. Such rejected data sets essentially suffer from a temporally varying PSF. However, unrejected data sets could have a temporally stable PSF and still have PSF-degraded color-aperture relationships.
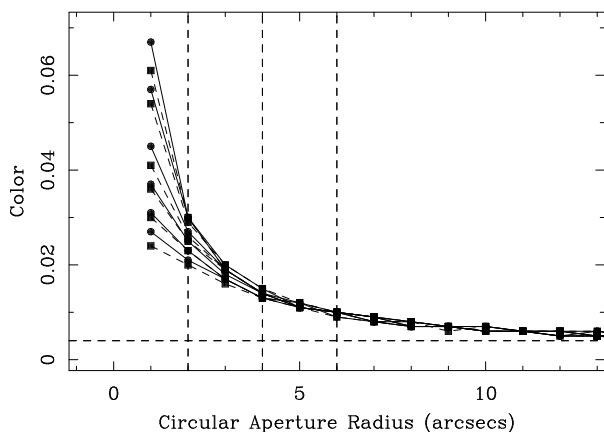

FIG. 1.—Simulated effects of varying PSF size and sampling on the measurement of an elliptical galaxy color-aperture relationship are shown. As discussed in § 3.2, an elliptical galaxy with a known color-aperture relationship was simulated. This simulation resulted in two images, one "red" and one "blue." These images were smoothed by circularly symmetric Gaussian PSFs with the following FWHM values: $0\overset{''}{.}5$, $1\overset{''}{.}0$, $1\overset{''}{.}5$, $2\overset{''}{.}0$, $2\overset{''}{.}5$, and $3\overset{''}{.}0$ (from top to bottom in the figure). PSF size is assumed to be equal in both photometric bands. The smoothed image pairs were then resampled on two different scales: $0\overset{''}{.}3$ pixel^{-1} (*circles connected by solid lines*) and $1\overset{''}{.}4$ pixel^{-1} (*squares connected by dashed lines*). The illustrated colors were measured from the smoothed, resampled image pairs through centered circular apertures. If color-aperture relationship determination were insensitive to sampling or PSF size, all curves in this figure would be the same. However, PSF size has a significant effect, while sample does not. Smaller PSF sizes produce more accurate color measurements within the smallest apertures, but PSF effects are negligible for larger apertures.

3.3. *Definition of Color Differences*

The semimajor axis of the central elliptical aperture for each galaxy was chosen to be $4''$–$5''$ (0.3–1.5 kpc). This choice is motivated by the following unavoidable compromise: On the one hand, we suspect that merger-induced star formation events will be quite centrally concentrated, so one wants to use the smallest possible aperture for detection. On the other hand, we have just demonstrated that the
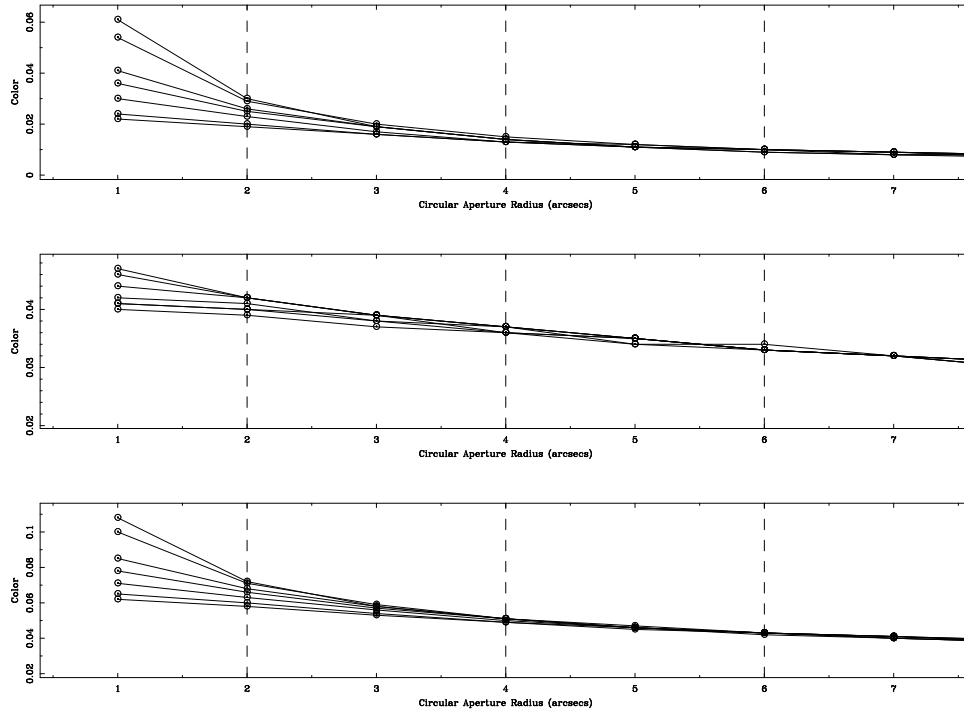
Fig. 2.—Simulated effects of varying PSF size on the measurement of color-aperture relationships for elliptical galaxies with different intrinsic color-aperture relationships are shown. The process described in Fig. 1 was repeated for three different color-aperture relationship types: increasing central reddening (*top*; repeat of Fig. 1 model), more shallow central reddening (*middle*), and central red source combined with shallow outer reddening (*bottom*). The Fig. 1 range of PSF FWHM size was also used here. Only the $1\rlap{.}''4$ pixel^{-1} models are shown. Varying PSF sizes have a much greater impact on color-aperture relationships with significant central color change (*top and bottom*) than on color-aperture relationships that are smooth at all radii (*middle*). See § 3.2 for further details.

redder the center of the color-aperture relationship, the more likely it is that a PSF difference exists. To be conservative, we have chosen a large enough central aperture size to minimize the possibility of introducing such a systematic error, which in turn means that detected color differences are likely to be lower estimates of the true color differences in these galaxies. The outer annuli were chosen to span the spatial semimajor axis range of $8\rlap{.}''5-11\rlap{.}''3$. This range is a
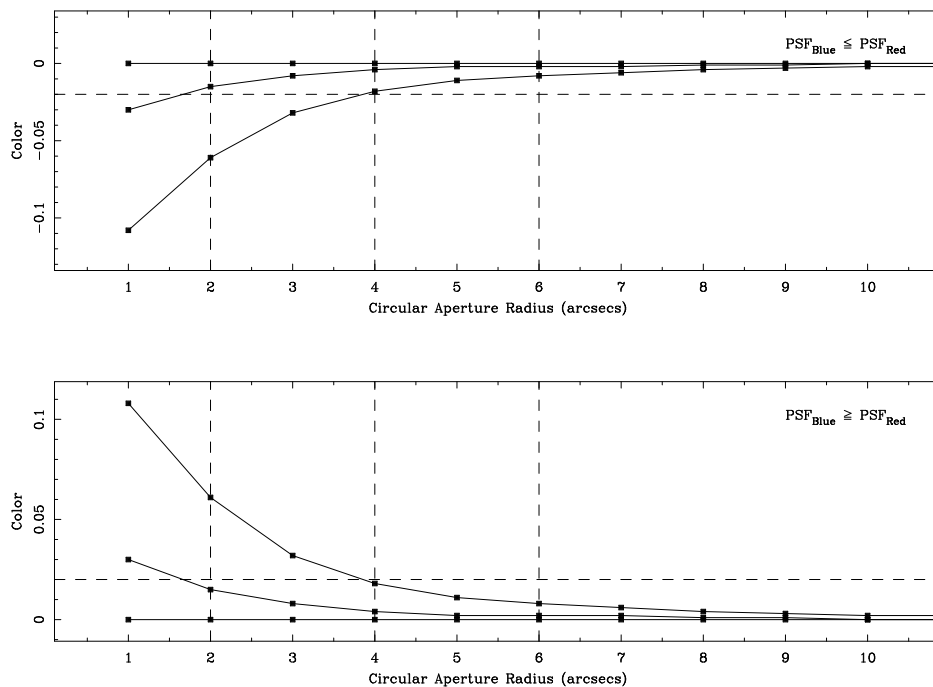

Fig. 3.—Effects of mismatched PSF sizes between photometric bands on a constant color-aperture relationship are illustrated. PSF size ratios of 1.0 (exact match, no effect), 1.1 (intermediate effect), and 1.3 (largest effect) are shown.

compromise between a large enough radius to have reached the part of the galaxy color-aperture relationship where color is approximately constant with increasing aperture and a small enough radial range to minimize background-driven color uncertainties.

For each galaxy, color differences between the central and outer regions, $\Delta(J-H)$ and $\Delta(H-K)$, were computed. *Positive* color differences mean a *redder* central region. These color difference have two error components. The first component is the background uncertainty σ_{bgnd}, discussed in § 2.2 of Paper I. The second component is a geometric uncertainty introduced by using the J elliptical isophotes to define rigidly the H and K isophotes, as discussed in § 3.1. The color uncertainty associated with this geometric uncertainty, σ_{geo}, was estimated using the following relationships:

$$J-K_0 = -2.5 \log \frac{F_J(r_2) - F_J(r_1)}{F_K(r_2) - F_K(r_1)}, \qquad (1a)$$

$$J-K^+ = -2.5 \log \frac{F_J(r_2 + 1) - F_J(r_1 + 1)}{F_K(r_2 + 1) - F_K(r_1 + 1)}, \qquad (1b)$$

$$J-K^- = -2.5 \log \frac{F_J(r_2 - 1) - F_J(r_1 - 1)}{F_K(r_2 - 1) - F_K(r_1 - 1)}, \qquad (1c)$$

where r_1 and r_2 are the inner and outer isophote semimajor axes of the isophotes that define the chosen annulus, $r_1 + 1$ and $r_2 + 1$ are the next outer isophotes, and $r_1 - 1$ and $r_2 - 1$ are the next inner isophotes. The standard deviation between $J-K_0$, $J-K_+$, and $J-K_-$ was assigned to σ_{geo}^{J-K}. Analogous equations can be written for $J-H$ and $H-K$. The final color difference uncertainty was then computed by summing the central and outer σ_{geo} and σ_{bgnd} in quadrature.

4. RESULTS

The resulting color differences and their uncertainties are listed in Table 2 and illustrated by Figure 4. Also shown in Figure 4 are vectors illustrating the effects of increasing metallicity (*solid line with stars*), increasing internal reddening (*dot-dashed line with squares*), and increasing fractional contribution of intermediate-age AGB light (*dashed line with squares*). The origin of these vectors, as well as a complete discussion of their applicability and reliability, is presented in Paper I.

4.1. *Galaxies with Small* $\Delta(H-K)$

We discuss galaxies with small $\Delta(H-K)$ first. Systematic errors caused by mismatched PSFs could easily cause color difference errors as large as ± 0.025 mag. The existence of some galaxies with $\Delta(H-K) < 0$ increases our suspicion that some of our data suffer from such systematic errors. In effect, $|\Delta(J-H)| \leq 0.025$ and $|\Delta(H-K)| \leq 0.025$ are consistent with *no* color difference. The simple increasing AGB light model presented in Paper I suggests that the centers of these galaxies must have no more than a 10% intermediate-age stellar mass enhancement per unit stellar mass relative to their outer regions, independent of their $\Delta(J-H)$. Given the large range in $\Delta(J-H)$, mean age is not the dominant astrophysical difference between the centers and outer regions of these elliptical galaxies. Some galaxies have $\Delta(J-H)$ consistent with either a central metallicity enhancement, which follows the Galactic globular cluster color-metallicity relationship, or with some small amount of increased internal reddening. We have begun acquiring
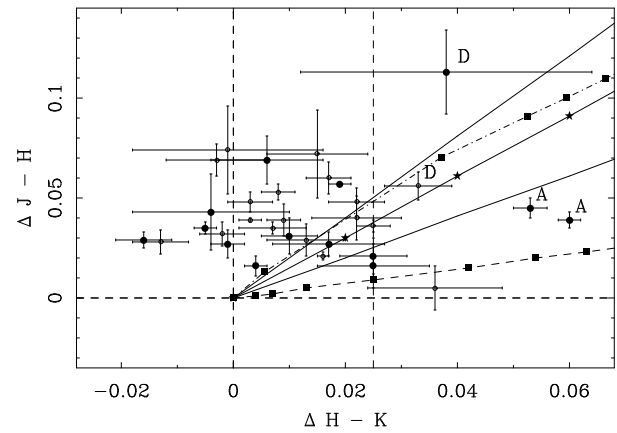

FIG. 4.—Color differences between the central region ($r \lesssim 0.5$ kpc) and an outer annulus ($1.0 \lesssim r \lesssim 1.5$ kpc) are shown. Positive color differences are equivalent to redder central regions. Error bars include random photometric errors and the geometric errors described in the text. "Young" elliptical galaxies with signs of recent merger activity are denoted by circles. Vectors illustrating the effects of increasing metallicity (*solid line with stars, range shown by solid lines without stars*), intermediate-age light (*dashed line with squares*), and internal reddening (*dot-dashed line with squares*) in the near-IR color-color plane are shown. Details about these vectors are given in Paper I. The two galaxies consistent with significant internal reddening due to dust, NGC 1052 and NGC 3921, are labeled "D." The two galaxies most consistent with a centrally concentrated intermediate-age stellar population, NGC 3610 and 5322, are labeled "A."

the requisite near-IR spectroscopic data needed to differentiate between these two possibilities.

About one-half of the galaxies in this group have $\Delta(J-H)$ values larger than implied by any of the vectors, even if they were all affected by the estimated typical systematic error [10%, or $\Delta(J-H) \sim 0.025$] caused by interband PSF differences. Although mean FGB temperature and metallicity are linearly correlated in Galactic globular clusters with [Fe/H] ≤ -0.3 (Aaronson et al. 1978), it is not certain what happens at higher metallicity. It does not appear, for example, that this combination of $\Delta(J-H)$ and $\Delta(H-K)$ can be caused by stars analogous to Baade's window (BW) giant branch stars, since the BW M giants are bluer in $J-H$ at a given $H-K$ than solar neighborhood M giants of similar $H-K$ color (Frogel & Whitford 1987; Tiede, Frogel, & Terndrup 1995), contrary to what is seen in our data.

On the other hand, consider the recently published near-IR color-color diagrams of Liller 1 and NGC 6440 (Frogel, Kuchinski, & Tiede 1995; Kuchinski & Frogel 1995). Liller 1 and NGC 6440 have [Fe/H] $= +0.25$ and -0.35, respectively. These clusters appear to have giant branches that are redder in $J-H$ than the giant branches of other clusters of similar metallicity. Do these unusual giant branches affect the integrated colors of these Galactic globular clusters? In the case of NGC 6440, the answer is yes. Compared with the integrated colors of other Galactic globular clusters of similar metallicity, NGC 6440 has similar $J-H$ color but very blue $H-K$ color (M. Malkan & M. Aaronson 1980, unpublished). In fact, the integrated $H-K$ color of NGC 6440 is consistent with the $H-K$ colors of clusters with [Fe/H] < -0.6. Equivalent large-aperture integrated colors for Liller 1 have not been published. If the centers of elliptical galaxies were dominated by a stellar population similar to NGC 6440, they could produce the kind of color changes seen in the galaxies

TABLE 2
CENTRAL COLOR DIFFERENCES

NGC (1)	$\Delta(J-H)$ (mag) (2)	$\sigma_{(J-H)}$ (mag) (3)	$\Delta(H-K)$ (mag) (4)	$\sigma_{(H-K)}$ (mag) (5)
315	0.028	0.006	−0.013	0.005
547	0.072	0.022	0.015	0.009
584	0.016	0.005	0.004	0.002
596	0.027	0.006	0.017	0.010
696	0.021	0.009	0.025	0.006
821	0.048	0.007	0.022	0.005
1023	0.021	0.002	0.016	0.001
1052	0.056	0.007	0.033	0.006
1172	0.074	0.022	−0.001	0.017
1453	0.029	0.008	0.013	0.007
1700	0.029	0.004	−0.016	0.005
2549	0.048	0.005	0.003	0.004
2685	0.035	0.003	0.007	0.006
2768	0.039	0.008	0.009	0.003
2974	0.036	0.003	0.025	0.003
3156	0.043	0.019	−0.004	0.014
3193	0.040	0.011	0.022	0.008
3377	0.031	0.009	0.010	0.005
3379	0.039	0.001	0.003	0.002
3489	0.060	0.008	0.017	0.004
3605	0.053	0.004	0.008	0.003
3608	0.069	0.008	−0.003	0.009
3610	0.039	0.004	0.060	0.002
3640	0.027	0.007	−0.001	0.003
3921	0.113	0.021	0.038	0.026
4125	0.035	0.003	−0.005	0.002
4168	0.005	0.011	0.036	0.012
4660	0.032	0.006	−0.002	0.004
4697	0.057	0.001	0.019	0.002
4915	0.016	0.011	0.025	0.010
5322	0.045	0.005	0.053	0.003
5831	0.069	0.012	0.006	0.010

NOTES.—Col. (1): NGC number. Col. (2): $J-H$ color difference between the central ($r \lesssim 0.5$ kpc) and an outer annulus ($1.0 \lesssim r \lesssim 1.5$ kpc). *Positive* numbers mean *redder* central regions. Col. (3): Uncertainty in $\Delta(J-H)$ computed as described in text. Col. (4): $H-K$ color difference between the central ($r \lesssim 0.5$ kpc) and an outer annulus ($1.0 \lesssim r \lesssim 1.5$ kpc). *Positive* numbers mean *redder* central regions. Col. (5): Uncertainty in $\Delta(H-K)$ computed as described in text.

that lie above the drawn vectors in Figure 4. A near-IR spectroscopic comparison between the M giant stars in NGC 6440 and Liller 1 and the centers of elliptical galaxies would be interesting.

4.2. *Galaxies with* $\Delta(H-K) > 0.025$

4.2.1. *Evidence for Central Internal Reddening*

Two galaxies with $\Delta(H-K) \geq 0.02$, NGC 1052 and NGC 3921 (labeled with "D" in Fig. 4), have central colors consistent with internal reddening. It is not surprising that NGC 1052 lies along the reddening vector in Figure 4, as strong dust features are observed in its nucleus (von Dokkum & Franx 1995), as well as at larger radii (Davies & Illingworth 1986).

The color differences within NGC 3921 are also likely to be caused by internal reddening. As discussed in Paper I, the global near-IR colors of this ongoing merger suggest that the near-IR light is dominated by old, metal-rich stars donated by the merger progenitors. However, the central near-IR colors of this nascent elliptical galaxy are redder than the outer region colors. The central optical colors are also significantly redder than the outer region colors (Schweizer 1996). This combination of redder optical and

near-IR colors rules out the possibility that the central region has a younger mean stellar age than the outer region. It also seems unlikely that this color effect is being caused by metallicity. If NGC 3921 was formed by an encounter between two bulge/disk systems, the bulges might have merged at the center of this proto–elliptical galaxy. Metallicity differences between the center and outer region of the should only be as great as the metallicity difference between spiral disks and bulges. While the magnitude of such disk/bulge metallicity differences is controversial (see, e.g., Terndrup et al. 1994; Peletier & Balcells 1996), the maximum difference appears to be 0.3 dex, i.e., a factor of ~ 2 smaller than the NGC 3921 color differences imply. Nor can the fading starburst population indicated by the presence of strong Balmer absorption lines be significantly contributing to the red near-IR light. Schweizer (1996) estimates that this population is ~ 1 Gyr old, too old to still be contributing young, red supergiants and too young to be contributing intermediate-age AGB stars. Thus, it seems most likely that the optical and near-IR color differences observed in NGC 3921 are caused by increased central internal reddening by dust. Although such central dust is seen in many elliptical galaxies (von Dokkum & Franx 1995; Carollo et al. 1997), its origin remains unclear.

4.2.2. *Evidence for Intermediate-Age Stars*

NGC 3610 also has $\Delta(H-K) > 0.025$, but here the central colors are consistent with the presence of intermediate-age AGB stars and a small amount of internal reddening. Additional observational support for such a population in NGC 3610 is provided by strong central Hβ absorption (Schweizer et al. 1990) and a nuclear mid-UV *HST* Faint Object Spectrograph spectrum that is similar to M32's and best matched by a mid-F main-sequence turnoff population (Spinrad et al. 1997). The central ($r \leq 4'' \approx 0.75$ kpc) region appears to have about 20%–30% more intermediate-age stellar mass per unit mass than its corresponding surrounding annulus, estimated using the simple increasing AGB light model presented in Paper I and accounting for a small amount of internal reddening ($A_V \approx 4$). This estimate of central intermediate-age fraction is consistent with the simple spectral synthesis analysis presented by de Jong & Davies (1997). Central gas, as traced by Hα + [N II] emission, has been detected (Goudfrooij et al. 1994). Such gas could be associated with dust as well. However, an archival *HST* Planetary Camera image of the center of NGC 3610 (Fig. 5) shows no evidence for dust, although it does reveal a complex central stellar structure that may be a ring or a twisted disk (see also Whitmore et al. 1997). The available *HST* images do not eliminate the possibility of a smoothly distributed dust component that could be causing significant internal reddening (Silva & Wise 1996).

NGC 5322 also has the red central near-IR colors and strong central Hβ absorption (Schweizer et al. 1990) suggestive of an intermediate-age stellar population. Like NGC 3610, it also has central gas, as traced by Hα + [N II] emission (Goudfrooij et al. 1994). Unlike NGC 3610, *HST* PC imagery of the center of NGC 5322 (Fig. 6) reveals a prominent central dust lane (first reported by von Dokkum & Franx 1995). Again, the available *HST* imagery does not eliminate the possibility of a distributed dust component causing significant internal reddening.

The near-IR colors of the central regions of these two galaxies suggest the presence of an intermediate-age stellar
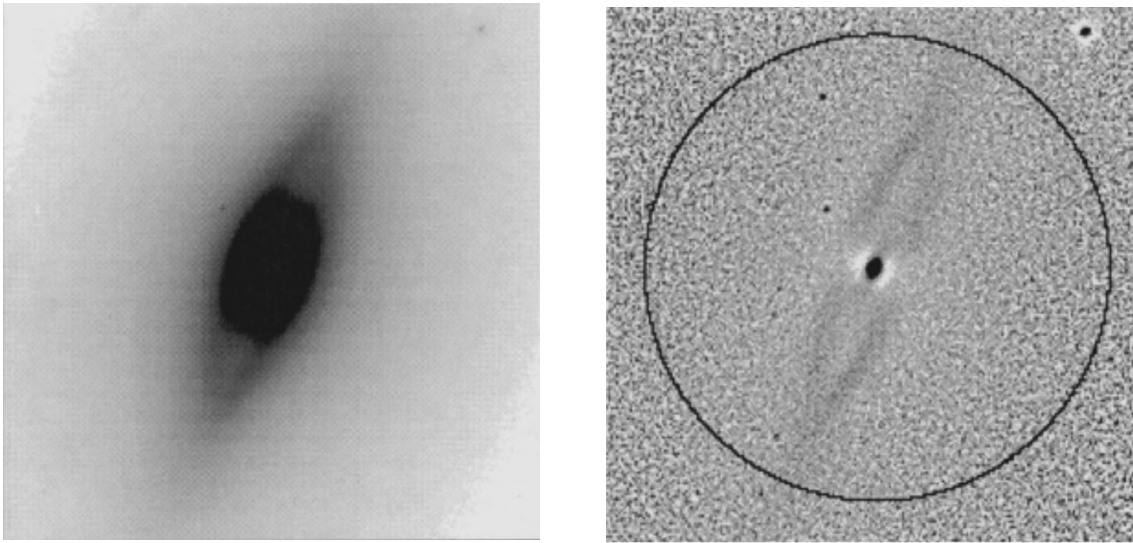
FIG. 5.—Central $9\farcs2 \times 9\farcs2$ region of NGC 3610, extracted from an archival *HST* Planetary Camera F555W image (*left*) and the same region after being divided by a Gaussian-smoothed (σ_{Gauss} = 2 pixels = $0\farcs092$) version of itself (*right*). *Darker* regions indicate *higher* intensity in both panels. A circle with $r = 4''$ is drawn on the right panel, corresponding to $r \approx 750$ pc for a distance of 39.1 Mpc ($H_0 = 50$; Bender, Burnstein, & Faber 1993). This delineates the "central region" used to construct the center − outer color differences. It is unclear whether the central structure illustrated in the right panel is the result of true stellar structure or if it is caused by "positive ringing" around the edges of a faint dust lane. Note, however, that this structure is seen in the left panel as well. The effects of "negative ringing" are illustrated in the right panel by the lighter regions around the galaxy nucleus and the foreground star in the upper right corner.

population that formed 1–3 Gyr ago. The global morphological structure of these galaxies is consistent with a merger event that occurred on about the same timescale. The obvious conclusion is that the young stars currently present in the centers of these galaxies were formed during the merger event. Indeed, the observed photoionization spectra suggest that residual star formation may be continuing in the centers of these galaxies, using gas left over from the initial merger event. We explore the implications of these observational conclusions further below.

5. DISCUSSION

5.1. *Commentary on the SS92 Study*

The key observational result of SS92 was that increased morphological fine structure is correlated with bluer optical colors, within the half-light radius, of their sample galaxies. This leads to a natural separation into two age bins: "intermediate-age" galaxies (2–7 Gyr old) with morphological fine structure and relatively blue colors and "old" (7–15 Gyr old) galaxies with relatively little morphological
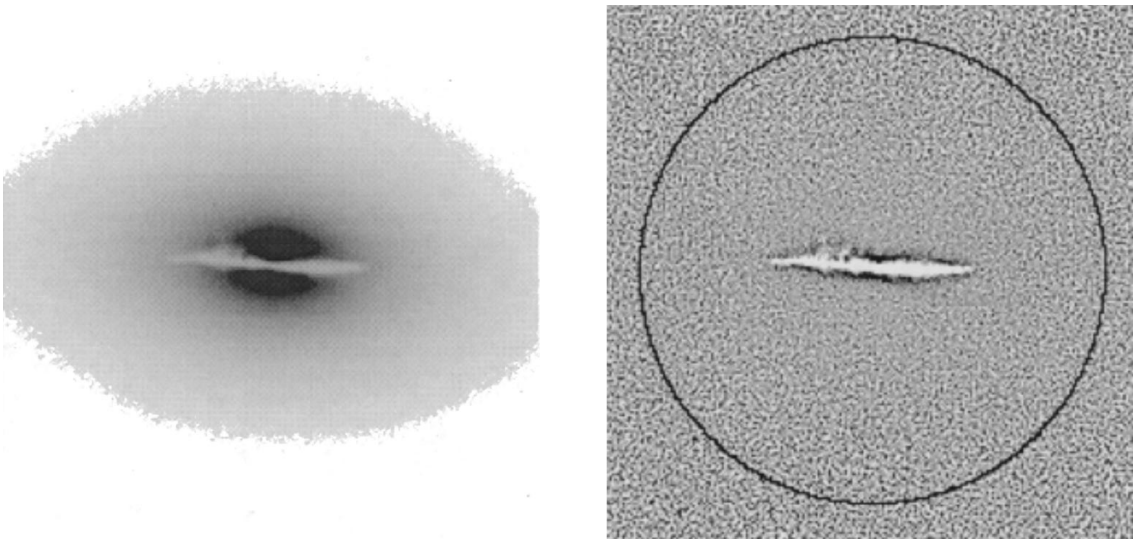

FIG. 6.—Central $9\farcs2 \times 9\farcs2$ region of NGC 5322, extracted from an archival *HST* Planetary Camera F555W image (*left*) and the same region after being divided by a Gaussian-smoothed (σ_{Gauss} = 1 pixel = $0\farcs046$) version of itself (*right*). *Darker* regions have *higher* intensity in both panels. A circle with $r = 4''$ is drawn on the right panel, corresponding to $r \approx 800$ pc for a distance of 42.1 Mpc ($H_0 = 50$; Bender et al. 1993). This delineates the "central region" used to measure the center − outer color differences. The dust lane seen in both panels was first reported by von Dokkum & Franx (1995). The dark border around the dust lane in the right panel is an artifact of the Gaussian smoothing process.

fine structure and red colors. They argued that global morphological and photometric properties of the intermediate-age galaxies were consistent with formation via recent disk-disk merging that mixed the "old" stellar component of the progenitor disk galaxies and created a "new" stellar component from the interstellar medium (ISM) of the progenitor disk galaxies. This intermediate-age stellar component must then affect the colors of the newly assembled galaxy within an effective radius. This is the signature that we looked for in the near-IR light of these galaxies.

The near-IR photometry presented in Paper I constrains the amount of intermediate-age stellar mass within the effective radius to 10% per unit mass and was consistent within the uncertainties with *no* intermediate-age stellar mass for the galaxies in our sample. This is consistent with models of disk-disk mergers that suggest that $\sim 5\%$ of the total remnant stellar mass could be tied up in younger stars (e.g., Mihos & Hernquist 1996). These young stars, however, should be centrally concentrated. However, with the key exceptions of NGC 3610 and 5322, the central ($r \lesssim 0.5$ kpc) near-IR colors presented here are inconsistent with such a centrally concentrated younger population.[4]

The lack of a significant (by mass) centrally concentrated young population appears to limit merger scenarios to events that did not involve gas, which in turn implies that galaxies akin to present-day spiral galaxies did not participate in these events. This drives us to consider unequal mass accretion event scenarios. Not only can such minor mergers produce the observed morphological fine structure, but as we discussed in Paper I, they can also lower the mean metallicity of the final galaxy relative to its progenitor and make them bluer relative to the galaxies of similar luminosity. This contradicts the conclusions of Schweizer et al. (1990) and González (1993) that increased central Hβ absorption indicates decreased luminosity-weighted mean age. Of our sample galaxies that have such increased central Hβ absorption, only NGC 3610 and 5322 have a central $H - K$ color consistent with a significant (by mass) intermediate-age stellar population. The central near-IR colors of the other galaxies are consistent with $\leq 10\%$ intermediate-age mass per unit mass within the central aperture.

In the extreme of no intermediate-age mass, the enhanced Hβ could originate from some combination of metallicity effects (both total metallicity and relative abundance changes; see Paper I) and horizontal-branch morphology. Currently published evolutionary synthesis stellar population models are not suitable for assessing these possibilities. Although evolutionary population synthesis workers face many challenges, we regard the reconciliation of the central near-IR colors and Hβ strengths to be one of the most important ones. We also note that detailed *HST* mid-UV nuclear spectroscopy of these galaxies would also be helpful (see discussion of NGC 3610 in Spinrad et al. 1997). Thus, although it is undeniable that disk-disk

mergers can and are forming proto–elliptical galaxies in the current epoch (e.g., NGC 3921 and 7252), it seems unlikely that most of the "intermediate-age" SS92 galaxies were formed in this fashion. NGC 5322 provides perhaps the *only* counterexample to this conclusion.

5.2. *Individual Case Studies*
5.2.1. *NGC 3610*

The spectacular morphological fine structure of NGC 3610 leads to the natural conclusion that this galaxy has undergone a recent merger event. This scenario is supported by the existence of a centrally concentrated intermediate-age stellar population, which is a prediction of the dissipative gas infall models. Furthermore, the central stellar structure seen in *HST* images (Fig. 5) could have been formed by this infalling gas. However, the global optical and near-IR colors of NGC 3610 constrain the amount of intermediate-age mass to less than 10% of the total mass and allow the possibility that there is no intermediate-age mass outside the central region (see Paper I). This is not necessarily inconsistent with the SS92 scenario. As they point out, during disk-disk mergers, most of the stellar mass is donated by the progenitor galaxies, not formed as part of the merger process, and is by definition older than the merger event. Furthermore, the models of Mihos & Hernquist (1996) suggest that any new stellar population formed during a disk-disk merger consists of $\sim 5\%$ of the final total remnant mass, well under our upper limit of 10%. Given that this mass could be very centrally concentrated, it is possible that it will not contribute a significant amount of flux to large-aperture measurements.

On the other hand, the stellar disk in NGC 3610, which extends well beyond its inner regions, provides a significant challenge to the disk-disk merger formation scenario. The disk and the bulk of the galaxy are closely aligned geometrically and have identical $V - I$ color (within 0.1 mag) (Scorza & Bender 1990).[5] The disk is also dynamically cold ($V_{\rm rot}/\sigma = 4$, at 2″) and corotates with the rest of the galaxy (Rix & White 1992). F555W and F814W images (i.e., $V - I$) of the center of NGC 3610 show that the central region ($r \lesssim 5″$) is *redder* than the surrounding galaxy by ~ 0.05 mag, which could be caused by stellar population effects or a diffuse dust component (Silva & Wise 1996; Wise & Silva 1998). The nuclear stellar structure seen in Figure 5 has the same color ($\sigma_{V-I} \approx 0.01$ mag) as the immediately surrounding light, although the actual nucleus may be bluer (cf. Whitmore et al. 1997). Confirming the latter will require a more careful analysis using detailed PSF deconvolution methods. Taken together, these photometric and dynamical features are quite consistent with coeval disk and bulge formation; i.e., there is no reason that the disk should have formed during a recent merger (cf. Rix & White 1992).

How then did the observed morphological features at large radii form? It seems unlikely that they were formed by a nonmerging tidal interaction (cf. Thomson & Wright 1990; Thomson 1991) since there is no nearby galaxy. A more plausible alternative scenario involves the accretion of a lower mass secondary galaxy (Quinn 1984; Dupraz & Combes 1986; Hernquist & Quinn 1988, 1989). Such

---

[4] Strictly speaking, the central and outer regions would also appear to be the same age in this method if *both* were dominated by an intermediate-age population. In that case, however, the global colors would also appear anomalous. NGC 221 = M32 exemplifies this effect: it has no central − outer color difference (Peletier 1993; Silva & Elston 1994) yet its global $H - K$ is clearly consistent with an intermediate-age stellar population (see Paper I). No galaxy in our sample exhibits both effects: no color difference but globally red $H - K$ colors.

[5] A $\Delta(V - I)$ uncertainty of 0.1 mag corresponds to an age uncertainty of ~ 3 Gyr at fixed metallicity ([Fe/H] = 0) and a metallicity uncertainty of ~ 0.3 dex at fixed age ($T = 12$ Gyr) (Worthey 1994).

encounters can create the outer morphological fine structure seen in NGC 3610 by redistributing the stars of the accreted companion. Since low-mass galaxies also tend to be bluer (and presumably more metal-poor), this redistribution would tend to make the colors of the final galaxy bluer than the original primary galaxy, as simulated photometrically in Paper I. Finally, if the accreted galaxy contained gas, that gas would dissipatively settle to the center, causing the formation of the inner stellar structure, the centrally concentrated younger stellar population, and the young globular cluster system reported by Whitmore et al. (1997).

We conclude that NGC 3610 was *not* assembled recently by a major disk-disk merger event within the last 3 Gyr, as suggested by SS92. It is more likely that the large-scale disk in NGC 3610 was formed long ago and recently survived a minor satellite accretion event. The central properties of this galaxy suggest that the accreted satellite contained significant amounts of gas. It is more likely that the relative global blueness of this galaxy is caused by metallicity effects, not age effects.

5.2.2. NGC 5322

NGC 5322 provides an interesting foil to NGC 3610. Like NGC 3610, NGC 5322 has photometric indicators of a central young population, as well as central gas and dust. The photometric and ISM features are spatially coincident with a central counterrotating kinematically decoupled core (KDC) (Bender 1988). This KDC may have slightly enhanced metallicity relative to the rest of the galaxy (Bender & Surma 1992), although not as much as seen in other KDC elliptical galaxies. However, the observed central dust lane may be blocking light from the most metal-rich component, lowering the luminosity-weighted mean KDC metallicity.

Based on isophotal properties, Bender (1988) suggested that the KDC in NGC 5322 was an inner disk. *HST* images of NGC 5322 (Fig. 6) reveal that the central isophotes are somewhat flattened and pointy but that the scale height is too large to be a cold disk (cf. Rix & White 1992). *HST* images also show that this central region becomes ~ 0.1 mag redder than the surrounding region. If this color change was a stellar population effect, this would imply $\Delta t \sim +3$ Gyr or $\Delta[\mathrm{Fe/H}] \sim +0.3$. The implied population difference is consistent with inferred spiral bulge/disk stellar population differences (Terndrup et al. 1994; Peletier & Balcells 1996), suggesting a model where the observed KDC was formed when the bulge components of the interacting progenitor spiral galaxies sank to the center of the potential well and merged. However, increased central age or metallicity is inconsistent with the near-IR data (see § 4.2.2), which suggests decreased central age coupled with increased internal reddening. It seems more likely that the observed $V-I$ reddening is caused by a small amount ($\lesssim 100\ M_\odot$) of smoothly distributed dust whose diffuse nature makes direct detection difficult but whose presence can still cause color gradients (see discussion in Silva & Wise 1996).

Given the observed optical and near-IR photometric properties, it seems unlikely that the KDC in NGC 5322 is merely a manifestation of dynamical streaming (Binney 1985; Franx, Illingworth, & de Zeeuw 1991; Statler 1994), which could create different dynamical features but not different photometric (i.e., stellar population) features. Rix & White (1992) have argued that the KDC in NGC 5322 is

dynamically hot enough ($V_{\mathrm{rot}}/\sigma = 1.4$) to be consistent with a dissipationless merger formation scenario (e.g., Balcells & Quinn 1990). However, counterrotating cores can also be formed by dissipational gasdynamical mechanisms (Hernquist & Barnes 1991; Barnes & Hernquist 1996). This latter mechanism seems more consistent with the observed stellar population and ISM properties. In short, a merger event involving gas could have created a younger, slightly more metal-rich KDC 1–3 Gyr ago which still contains residual dust and gas today. Was this gasdynamical event part of a disk-disk merger event, as suggested by SS92?

Although the core properties seem consistent with this conclusion, it is the additional broadband optical blue light at larger radii that remains a problem. Even if the merger event formed a younger population, all published models indicate that this population will be centrally concentrated, not distributed throughout the volume delineated by the effective radius. Although some young stars may be distributed more globally via splashback of tidal debris (see, e.g., Hibbard & Mihos 1995), the luminosity-weighted contribution of such stars will be quite small. Thus, it seems unlikely that the extra-blue global blue light is driven by age. Metallicity effects are the obvious alternative origin of this blue light. As discussed in detail in Paper I, NGC 5322 could be bluer than galaxies of similar blue luminosity either because it has accreted a more metal-poor companion (a minor accretion event) or because it has a lower [Mg/Fe] due to a disk-disk merger (Bender 1996). We conclude that while the central photometric and spectroscopic properties of NGC 5322 are driven by a combination of age and internal reddening, the global photometric properties (i.e., its relatively blue color) are driven by metallicity effects and not age.

5.3. The Many Ages of Field Elliptical Galaxies

The epoch and process of galaxy formation remain ambiguous largely because we have yet to observe it. As a result, it is still quite common to discuss the age of elliptical galaxies as if this were a single-valued number. This concept is tied to the hypothesis that the vast majority of elliptical galaxies formed from a single collection of gas at high redshift, and thereafter their stellar populations and dynamical properties evolved passively. Recent observations suggest a considerably more complicated formation. On the one hand, the morphology of objects in the Hubble Deep Field suggests that galaxy formation is an extended process that requires galaxy assembly from a production line of building blocks of subgalactic size (e.g., Pascarelle et al. 1996). On the other hand, there is definitive evidence (e.g., Steidel et al. 1996) for the existence of star-forming galaxies at $z \sim 3.5$. Furthermore, there are genuine examples of old galaxies at redshifts greater than 1.5 (Dunlop et al. 1996; Spinrad et al. 1997). Indeed, based on the evolution of QSO metal line strengths with redshift (Steidel 1992), there is clear evidence of a rapid increase in mean metallicity of gas between $z = 4$ and $z = 2$. All of these conditions suggest that some star formation in spheroids begins at $z \sim 4$ but that the amount of star formation shows considerable variation. In that sense, the concept of a mean age of a galaxy reflects much more than just the beginnings of the formation process. Cumulative environmental influences between $z \sim 4$ and $z \sim 1$ are likely to play a more dominant role.

What constraints are provided by the current study? An executive summary would state that present-day elliptical

galaxies are most likely not built by major mergers of disks at $z < 1$. However, our data cannot really constrain the assembly age of these galaxies. As SS92 (among others) have pointed out, the presence of an old stellar population does not imply an old assembly age. In hierarchical models of galaxy formation, galaxy assembly in low-density environments can continue indefinitely, albeit at an ever decreasing rate (see e.g., Toomre 1977; White & Rees 1978; Blumenthal et al. 1984). Since the subgalaxy building blocks formed their stars at high redshift and then merged to form the larger units seen in the current epoch quite recently, the stellar mass can be quite old while the galaxy is relatively young. Recent unequal mass merger/accretion events may just be the tail end of the field galaxy assembly process. Our data strongly argue that this assembly process has not been active for the last few gigayears. Indeed, our sample galaxies have a mass-weighted mean stellar age of at least 5 Gyr. Furthermore, the last significant star formation event (i.e., an event involving 10% of the current stellar mass) was longer ago than 3 Gyr. The lack of a significant centrally concentrated intermediate-age population in most of the elliptical galaxies with significant morphological fine structure suggests that their most recent mergers did not involve a significant amount of gas and therefore did not involve galaxies akin to current-epoch spiral galaxies.[6]

It is tempting to conclude that the available observational evidence indicates that the stellar populations of field elliptical galaxies were formed and assembled into their current dynamical ensemble at high redshift and that recent ($t \lesssim 5$ Gyr) epoch mergers have been relatively minor, i.e., did not involve major disk-disk mergers. However, it is not really possible to reconcile this conclusion with the Kauffmann, Charlot, & White (1996) result that suggests that 50%–70% of the current-epoch field E/S0 galaxies were assembled at $z \lesssim 1$. Unless the major assembly epoch was between $z = 0.5$ and 1.0, our near-IR observations would detect this process. We do note that the current literature abounds (e.g., Im & Casertano 1998 and references therein) with contradictory claims about the evolutionary rate of E/S0 galaxies between $z = 0$ and 1. We believe that our data strongly suggest little activity in this regard since $z \sim 0.5$.

6. SUMMARY

1. Regardless of their global morphological fine structure, most of the galaxies in our samples have central colors consistent with increased metallicity and/or internal reddening, relative to their outer regions, not decreased mean age as a result of a centralized star formation event a few gigayears ago.

2. Two galaxies, NGC 3610 and 5322, have central near-IR colors consistent with the presence of an intermediate-age stellar population. We conclude that these

galaxies have undergone a merger-driven central star formation event roughly 1–3 Gyr ago.

3. In contrast to SS92, however, we conclude that few of these morphologically disturbed elliptical galaxies were formed by mergers of disk galaxies akin to current-epoch spiral galaxies in the last 3–5 Gyr. This conclusion is based primarily on the lack of centrally concentrated AGB light in these elliptical galaxies. We also conclude that metallicity effects, not age effects, are likely to be the primary source of the excess blue light seen within the effective radii of these galaxies.

4. While we have emphasized that most ($>90\%$) of the stellar mass in these galaxies must be old ($T > 10$ Gyr) and metal-rich ([Fe/H] ≥ -0.3), we also emphasize that the nature of the stars does not constrain the assembly age of these elliptical galaxies. This problem affects all similar studies of the photometric and spectroscopic properties of elliptical galaxies.

We close with a few simple remarks about interpreting the stellar populations of recent merger products at higher redshift. If gas is involved, dissipation will drive most of it to the center of the potential well. It is only there that star formation and, subsequently, relative age differences are important. This younger population, however, will not typically affect the global galaxy color after the initial starburst. It will be nearly impossible to measure accurate colors and line indices in the inner 0.5 kpc of these distant galaxies until much larger aperture space-based telescopes are available. For the foreseeable future, spectrophotometric measurements will be dominated by the light coming from larger radii. At these larger radii, the dissipationless redistribution of stellar mass throughout the potential well will create photometric signatures that are metallicity-driven, not age-driven. For high-luminosity postmerger neo–elliptical galaxies in low-density environments at $z \gtrsim 0.5$, it may be these metallicity effects that drive the observable photometric evolution, not age effects. Testing the validity of this statement presents a major challenge for understanding the photometric evolution of early-type galaxies in low-density environments. As we have demonstrated, acquisition of rest-frame near-IR data can provide crucial constraints.

---

[6] Bender (1996) has also argued that it is unlikely that most luminous elliptical galaxies have formed from the mergers of spiral galaxies because while spiral galaxies have [Mg/Fe] ~ 0, luminous elliptical galaxies have [Mg/Fe] $= 0.3$–0.4. In short, the input stellar populations of spiral galaxies cannot reproduce the observed integrated spectral features of luminous elliptical galaxies.

REFERENCES

Aaronson, M., Cohen, J. G., Mould, J., & Malkan, M. 1978, ApJ, 223, 824
Balcells, M., & Quinn, P. J. 1990, ApJ, 361, 381
Barnes, J. E. 1992, ApJ, 393, 984
Barnes, J. E., & Hernquist, L. 1991, ApJ, 370, L65
———. 1996, ApJ, 471, 115
Bender, R. 1988, A&A, 202, L5
———. 1996, in New Light on Galaxy Evolution, ed. R. Bender & R. L. Davies (Dordrecht: Kluwer), 181
Bender, R., Burstein, D., & Faber, S. M. 1993, ApJ, 411, 135
Bender, R., & Surma, P. 1992, A&A, 258, 250
Bender, R., Surma, P., Döbereiner, S., Möllenhoff, C., & Madejsky, R. 1989, A&A, 217, 35
Binney, J. 1985, MNRAS, 212, 767
Blumenthal, G., Faber, S. M., Primack, J., & Rees, M. J. 1984, Nature, 311, 517
Burstein, D., Davies, R. L., Dressler, A., Faber, S. M., Stone, R. P. S., Lynden-Bell, D., Terlevich, R. J., & Wegner, G. 1987, ApJS, 61, 601
Burstein, D., & Heiles, C. 1984, ApJS, 54, 33
Carollo, C. M., Franx, M., Illingworth, G. D., & Forbes, D. A. 1997, ApJ, 481, 710
Davies, R. L., Burstein, D., Dressler, A., Faber, S. M., Lynden-Bell, D., Terlevich, R. J., & Wegner, G. 1987, ApJS, 64, 581
Davies, R. L., & Illingworth, G. D. 1986, ApJ, 302, 234
de Jong, R. S., & Davies, R. L. 1997, MNRAS, 285, L1
Downes, D., & Solomon, P. M. 1998, ApJ, in press
Dunlop, J., Peacock, J., Spinrad, H., Dey, A., Jimenez, R., Stern, D., & Windhorst, R. 1996, Nature, 381, 581
Dupraz, C., & Combes, F. 1986, A&A, 166, 53
Elias, J. H., Frogel, J. A., Matthews, K., & Neugebauer, G. 1982, AJ, 87, 1029
Ellis, T., et al. 1993, Proc. SPIE, 1765, 94
Faber, S. M., Tremaine, S., Ajhar, E., Byun, Y.-I., Dressler, A., Gebhardt, K., Grillmar, C., & Kormendy, J. 1997, AJ, 114, 1771
Franx, M., Illingworth, G., & de Zeeuw, T. 1991, ApJ, 383, 112
Franx, M., Illingworth, G., & Heckman, T. 1989, ApJ, 344, 613
Frogel, J. A., Kuchinski, L. E., & Tiede, G. P. 1995, AJ, 109, 1154
Frogel, J. A., Mould, J., & Blanco, V. M. 1990, ApJ, 352, 90
Frogel, J. A., & Whitford, A. E. 1987, ApJ, 320, 199
González, J. J. 1993, Ph.D. thesis, Univ. California, Santa Cruz
Goudfrooij, P., Hansen, L., Jørgensen, H. E., & Nørgaard-Nielsen, H. U. 1994, A&AS, 105, 341
Hernquist, L., & Barnes, J. E. 1991, Nature, 354, 210
Hernquist, L., & Quinn, P. J. 1988, ApJ, 331, 682
———. 1989, ApJ, 342, 1
Hibbard, J. E., & Mihos, J. C. 1995, AJ, 110, 140
Illingworth, G. D., & Franx, M. 1989, in Dynamics of Dense Stellar Systems, ed. D. Merritt (Cambridge: Cambridge Univ. Press), 13
Im, M., & Casertano, S. 1998, ApJ, submitted

Jedrzejewski, R. I. 1987, MNRAS, 226, 747
Kauffmann, G., Charlot, S., & White, S. D.M. 1996, MNRAS, 283, L117
Kuchinski, L. E., & Frogel, J. A. 1995, AJ, 110, 2844
Mihos, J. C., & Bothun, G. D. 1998, ApJ, 500, 619
Mihos, J. C., Bothun, G. D., & Richstone, D. O. 1993, ApJ, 418, 82
Mihos, J. C., & Hernquist, L. 1996, ApJ, 464, 641
Negroponte, J., & White, S. D. M. 1983, MNRAS, 205, 1009
Pascarelle, S., Windhorst, R., Keel, W., & Odewahn, S. 1996, Nature, 383, 45
Peletier, R. F. 1993, A&A, 271, 5
Peletier, R. F., & Balcells, M. 1996, AJ, 111, 2238
Peletier, R. F., Davies, R. L., Davis, L. E., Illingworth, G. D., & Cawson, M. 1990, AJ, 100, 1091
Persson, S. E., Aaronson, M., Cohen, J. G., Frogel, J. A., & Matthews, K. 1983, ApJ, 266, 105
Quinn, P. J. 1984, ApJ, 279, 596
Rix, H.-W., & White, S. D. M. 1992, MNRAS, 254, 389
Sandage, A., & Tammann, G. A. 1981, A Revised Shapley-Ames Catalog of Bright Galaxies (Washington: Carnegie Inst. Washington)
Schweizer, F. 1996, AJ, 111, 109
Schweizer, F., & Seitzer, P. 1992, AJ, 104, 1039 (SS92)
Schweizer, F., Seitzer, P., Faber, S. M., Burstein, D., Dalle Ore, C. M., & Gonzalez, J. J. 1990, ApJ, 364, L33
Scorza, C., & Bender, R. 1990, A&A, 235, 49
Silva, D. R., & Bothun, G. D. 1998, AJ, 116, 85 (Paper I)
Silva, D. R., & Elston, R. 1994, ApJ, 428, 511
Silva, D. R., & Wise, M. W. 1996, ApJ, 457, L15
Spinrad, H., Dey, A., Stern, D., Dunlop, J., Peacock, J., Jimenez, R., & Windhorst, R. 1997, ApJ, 484, 581
Statler, T. S. 1994, ApJ, 425, 458
Steidel, C. C. 1992, Ph.D. thesis, Univ. California, Berkeley
Steidel, C. C., Giavalisco, M., Pettini, M., Dickinson, M., & Adelberger, K. L. 1996, ApJ, 462, L17
Terndrup, D. M., Davies, R. L., Frogel, J. A., DePoy, D. L., & Wells, L. A. 1994, ApJ, 432, 518
Thomson, R. C. 1991, MNRAS, 253, 256
Thomson, R. C., & Wright, A. E. 1990, MNRAS, 247, 122
Tiede, G. P., Frogel, J. A., & Terndrup, D. M. 1995, AJ, 110, 2788
Toomre, A. 1977, in The Evolution of Galaxies and Stellar Populations, ed. B. M. Tinsley & R. B. Larson (New Haven: Yale Univ. Press), 401
van Dokkum, P. G., & Franx, M. 1995, AJ, 110, 2027
White, S. D. M., & Rees, M. J. 1978, MNRAS, 183, 341
Whitmore, B. C., Miller, B. W., Schweizer, F., & Fall, S. M. 1997, AJ, 114, 1797
Wise, M. W., & Silva, D. R. 1998, ApJ, submitted
Worthey, G. 1994, ApJS, 95, 10
Worthey, G., Faber, S. M., & Gonzalez, J. J. 1992, ApJ, 398, 69